

The evolution of galaxy clustering

J.A. Peacock

Royal Observatory, Blackford Hill, Edinburgh EH9 3HJ

ABSTRACT

This paper investigates whether nonlinear gravitational instability can account for the clustering of galaxies on large and small scales, and for the evolution of clustering with epoch. The local clustering spectrum is accurately established, and bias is not a great source of uncertainty: the real-space power spectra of optical and IRAS galaxies show only a weak scale-dependent relative bias of $b \simeq 1.15$ on large scales, increasing to $b \simeq 1.5$ on the smallest scales. Comparison with results in redshift space favours a relatively small distortion parameter $\beta_{\text{opt}} \equiv \Omega^{0.6}/b_{\text{opt}} \simeq 0.4$.

No CDM-like spectrum is consistent with the shape of the observed nonlinear spectrum. Unbiased low-density models greatly overpredict the small-scale correlations; high-density models would require a bias which does not vary monotonically with scale. The true linear power spectrum contains a primordial feature at $k \simeq 0.1 h \text{ Mpc}^{-1}$, and must break quite abruptly to an effective slope of $n \lesssim -2.3$ on smaller scales.

This empirical fluctuation spectrum also fits the CFRS data on the evolution of clustering, provided the universe is open with $\Omega \simeq 0.3$. Only this case explains naturally how the small-scale spectrum can evolve at the observed rate while retaining the same power-law index. An unbiased open model also matches correctly the large-scale COBE data, and offers an attractively simple picture for the phenomenology of galaxy clustering.

Key words: galaxies: clustering – cosmology: theory – large-scale structure of Universe.

1 INTRODUCTION

Studies of galaxy clustering have progressed steadily towards measurements on ever larger scales. The influential text by Peebles (1980) could call only on results from angular clustering in the Lick survey, which established the power-law form of the correlation function at separations $\lesssim 10 h^{-1} \text{ Mpc}$ ($h \equiv H_0/100 \text{ km s}^{-1} \text{ Mpc}^{-1}$). The following years have yielded a succession of larger and deeper redshift surveys which probe clustering well into the linear regime at separations approaching $100 h^{-1} \text{ Mpc}$ (e.g. CfA1: Davis & Peebles 1983; CfA2: de Lapparent et al. 1986; IRAS QDOT: Saunders et al. 1991; IRAS 1.2-Jy: Fisher et al. 1993; APM-Stromlo: Loveday et al. 1992).

These later studies have concentrated on the shape of the large-scale fluctuation spectrum, for two main reasons: (1) the shape of the linear spectrum allows a test of fundamental models for the generation of fluctuations, plus the modifying effects of dark matter; (2) redshift-space distortions mean that redshift surveys provide a highly distorted measure of clustering at separations $\lesssim 1 h^{-1} \text{ Mpc}$. As long as there was uncertainty over the form of large-scale clustering, it therefore made sense to keep the focus in this area. However, a comparison of various large-scale measurements by Peacock & Dodds (1994; PD94) suggested that the shape of the clustering power spectrum for wavenumbers $k \lesssim 0.3 h \text{ Mpc}^{-1}$ was being measured consistently by a variety of galaxy tracers. One aim of the present paper is

therefore to concentrate on the small-scale data, to see how extending the range of the clustering spectrum narrows the possible interpretations of the data.

A further development which makes it timely to concentrate on non-linear clustering is the evolution of the galaxy correlation function. The angular clustering of faint galaxies has long indicated changes in $\xi(r)$ with epoch (e.g. Efsthathiou et al. 1991; Neuschaefer, Windhorst & Dressler 1991; Couch et al. 1993; Roche et al. 1993), but a more direct measurement has recently been made by the Canada-France Redshift Survey (Le Fèvre et al. 1996), which yields spatial clustering in different redshift bins up to $z = 1$. Although a variety of different models are capable of accounting for the local clustering data, these alternatives make different predictions for the change in clustering with epoch; the second aim of the present paper is therefore to combine the CFRS measurements with the data on clustering at $z = 0$, and to ask if any model can successfully account for both.

The plan of the paper is as follows. Section 2 assembles the data on the real-space clustering of optical and IRAS galaxies, and considers their relative bias and degrees of redshift-space distortion. Section 3 reviews analytical methods for obtaining nonlinear power spectra, and proposes some empirical models which can explain the data. Section 4 explores the predictions for the evolution of clustering in these models, in comparison with the CFRS data. Section 5 adds the requirement of consistency with fluctuations in the cosmic microwave background (CMB). Section 6 sums

up the conclusions of these studies, which suggest that a low-density open universe with a small degree of bias is the line of least resistance.

2 THE CLUSTERING OF OPTICAL AND IRAS GALAXIES

2.1 Clustering in real space

It is not wise to assume in advance that any given class of galaxy traces cosmological density in an unbiased fashion, and we should therefore look at the properties of a variety of tracers. Two interesting cases for which the best data exist are optically-selected galaxies and IRAS galaxies. Since we are interested in clustering at small separations, it is necessary to use real-space results. For optical galaxies, the best power-spectrum determination is from the angular correlations of the APM survey (Maddox et al. 1990; 1996), as deprojected by Baugh & Efstathiou (1993; 1994). For IRAS galaxies, the best available result is from the cross-correlation between the 1-in-6 QDOT survey and its parent catalogue (Saunders, Rowan-Robinson & Lawrence 1992). To reduce the data to accurate estimates of the real-space power spectra for optical and IRAS galaxies requires a number of steps, which are detailed below. The resulting power spectra are shown in Figure 1, where we follow PD94 in using a dimensionless notation for the power spectrum: Δ^2 is the contribution to the fractional density variance per bin of $\ln k$. In the convention of Peebles (1980), this is

$$\Delta^2(k) \equiv \frac{d\sigma^2}{d \ln k} = \frac{V}{(2\pi)^3} 4\pi k^3 |\delta_k|^2, \quad (1)$$

and the relation to the correlation function is

$$\xi(r) = \int \Delta^2 \frac{dk}{k} \frac{\sin kr}{kr}. \quad (2)$$

A dominant topic in PD94 was how to correct redshift-survey data for the distorting effects of peculiar velocities on the radial coordinate; however, a variety of projection schemes exist whereby the real-space correlations may be obtained in an unbiased manner. Saunders et al. (1992) used the angular cross-correlation between the QDOT redshift survey and its (larger) parent catalogue to obtain the projected correlation function

$$\Xi(r) = \int_{-\infty}^{\infty} \xi[(r^2 + x^2)^{1/2}] dx = 2 \int_r^{\infty} \xi(y) \frac{y dy}{\sqrt{y^2 - r^2}}. \quad (3)$$

At first sight, it is not very attractive to use this to infer the power spectrum, because the window function involved is extremely broad:

$$\frac{1}{r} \Xi(r) = \int \Delta^2(k) \frac{dk}{k} \left[\frac{\pi}{kr} J_0(kr) \right]. \quad (4)$$

Fortunately, Saunders et al. inverted the integral relation between Ξ and ξ and then converted ξ to a variance in cubical cells of side ℓ , which is readily converted to the power at an effective wavenumber, as discussed by Peacock (1991):

$$\sigma^2(\ell) = \Delta^2(k_{\text{eff}}). \quad (5)$$

For power-law spectra, $\Delta^2 \propto k^{n+3}$, with $-2 \lesssim n \lesssim 0$, $\sigma^2(\ell)$ approximately measures $\Delta^2(2.4/\ell)$, and the effective

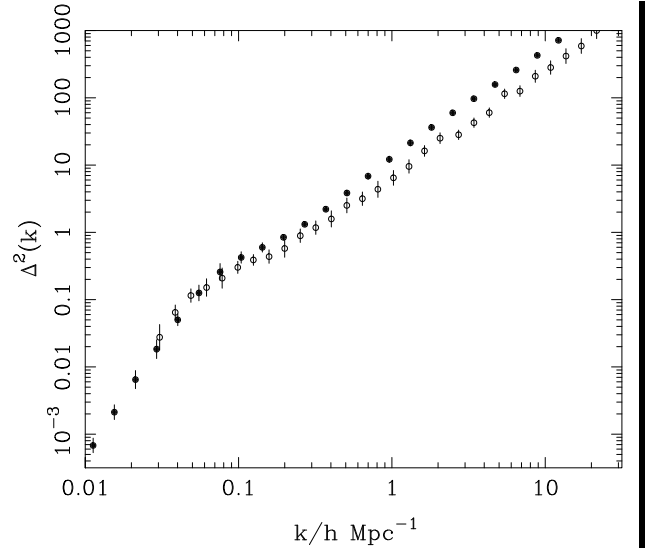


Figure 1. The real-space power spectra of optically-selected APM galaxies (solid circles) and IRAS galaxies (open circles), obtained from the references given in the text. Except possibly on the very largest scales, IRAS galaxies show weaker clustering, consistent with their suppression in high-density regions relative to optical galaxies.

wavenumber can be determined even more precisely by performing the integral for $\sigma^2(\ell)$ over a smoothly-curving spectrum of the observed form.

The plot in Saunders et al. (1992) which contains $\sigma^2(\ell)$ does not extend to very small scales, but we can recover the power spectrum in this regime because the small-scale correlations are very close to a single power law. Consider the projected correlations and power spectra for a correlation function of the form $\xi = [r/r_0]^{-\gamma}$:

$$\frac{1}{r} \Xi(r) = \frac{\Gamma(1/2)\Gamma([\gamma-1]/2)}{\Gamma(\gamma/2)} [r/r_0]^{-\gamma}. \quad (6)$$

$$\Delta^2(k) = \frac{2}{\pi} \Gamma(2-\gamma) \sin \frac{(2-\gamma)\pi}{2} [kr_0]^\gamma. \quad (7)$$

These relations suggest an equivalent wavenumber $\Xi(r)/r = \Delta^2(k_{\text{eff}})$, where $k_{\text{eff}} = 3.055/r$ for the $\gamma = 1.57$ slope characteristic of the small-scale IRAS correlation function. The IRAS power spectrum from the Saunders et al. (1992) paper is therefore based on this method for $k \gtrsim 1 h \text{ Mpc}^{-1}$ and on $\sigma^2(\ell)$ for larger scales; the two techniques match very well where they join.

The real-space power spectrum for optically-selected galaxies is available in a much more direct form from the work of Baugh & Efstathiou (1993, 1994). They inverted the integral equations relating the angular correlation function and the angular power spectrum to the spatial power spectrum. The results from the first of these papers were used in PD94. Before using them here, however, it is advisable to make one small correction. The Baugh & Efstathiou formalism incorporates evolution of clustering with redshift, but their standard results are quoted assuming no evolution. Since the median redshift of the $17 < B < 20$ samples they analyze is close to 0.2, this can lead to a significant under-estimate of the zero-redshift correlations. This can

be checked against the recent results of the APM-Stromlo $B < 17$ redshift survey team. Loveday et al. (1995) applied the projection technique of Saunders et al. (1992) to deduce that $\xi = [r/5.1 h^{-1} \text{Mpc}]^{-1.71}$ for optically selected galaxies. Fourier transforming the Baugh & Efstathiou power spectrum yields a correlation function which is uniformly lower than this by a factor of approximately 0.8 over to range $1 - 10 h^{-1} \text{Mpc}$, and so we have re-scaled the power spectrum to correct for this factor. The results produced in this way are essentially identical to those given in Maddox et al. (1996), where the deprojection was performed allowing for evolution. The errors in Baugh & Efstathiou (1993) are smaller on large scales than those given by Maddox et al. (1996), even though both are supposedly based on field-to-field scatter. To be conservative, the larger errors were adopted.

2.2 Optical-to-IRAS bias

Figure 1 shows the well-known result that IRAS galaxies cluster less strongly than optical galaxies. At least one of these classes of galaxy must therefore be biased with respect to the mass. The *relative* bias as a function of scale can be defined as the square root of the ratio of the power spectra. This is shown in Figure 2. For the smallest scales, the relative bias is about 1.5, but this declines with scale, reaching a plateau at $b_{\text{opt}}/b_{\text{IRAS}} \simeq 1.1$ around $k \simeq 0.1 h \text{Mpc}^{-1}$, before declining rather abruptly below 1 on larger scales. For $k \lesssim 0.05 h \text{Mpc}^{-1}$, according to these data, IRAS galaxies appear to be more clustered than optical galaxies. This is a suspicious feature, both for its sudden onset and because the known suppression of IRAS galaxies in high-density regions would lead us to expect IRAS galaxies to be less strongly clustered on all scales. Apart from this last feature, the striking feature of the plot is the slowly-varying nature of the relative bias, and it would be useful to describe this by a fitting formula.

A reasonable form to try is something which is a combination of linear bias and a non-linear response for $\Delta^2 \gtrsim 1$:

$$1 + \Delta_{\text{opt}}^2 = [1 + b_1 \Delta_{\text{IRAS}}^2]^{b_2}. \quad (8)$$

Mann, Peacock & Heavens (1996) show that this is a practical form for describing many empirically reasonable forms of bias. Local modifications of N -body density fields such as suppressing particles in low-density voids or weighting up particles in clusters produce a scale dependence which can be fitted by this form. The behaviour is always monotonically increasing towards small scales, as proved on rather general grounds for all local bias schemes by Coles (1993). The scale dependence can often be relatively weak, as is the case here, and the observed relative bias of optical and IRAS galaxies is therefore very much the sort of thing that would be expected from the known enhancement of optical galaxies relative to IRAS galaxies in high-density regions (Strauss et al. 1992).

The best-fitting parameters in this formula are

$$\begin{aligned} b_1 &= 1.17 \pm 0.10 \\ b_2 &= 1.13 \pm 0.01, \end{aligned} \quad (9)$$

so that the linear bias parameter in the long-wavelength regime would be

$$b = [b_1 b_2]^{1/2} = 1.15 \pm 0.05. \quad (10)$$

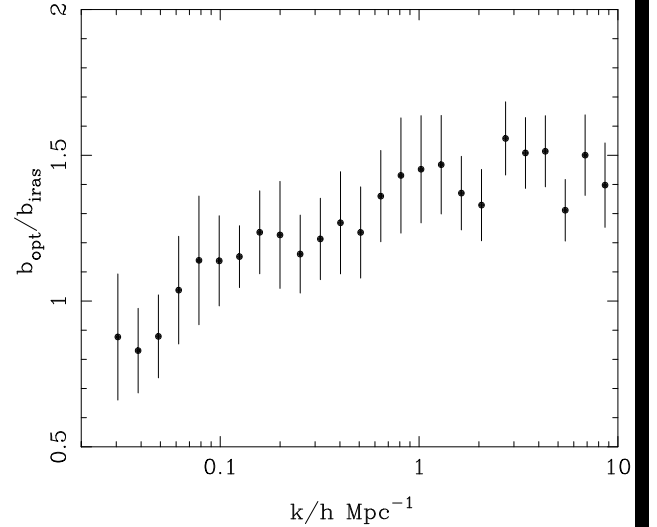


Figure 2. The relative bias of optical galaxies relative to IRAS galaxies as a function of wavenumber, obtained from the square root of the ratio of the power spectra in Fig. 1. The large-scale bias takes values between 1.1 and 1.2 over a decade in scale, $0.06 \lesssim k \lesssim 0.6 h \text{Mpc}^{-1}$, before breaking sharply to values < 1 on larger scales.

Much the same result is obtained whether the whole range of the data is used, or whether the large-scale points with $b < 1$ are omitted. Because the relative bias is nearly a constant in the region of 1.2 over a large range of k , this says that it is indeed implausible that the large-scale points with $b < 1$ can be correct.

Figure 3 shows the results of scaling the IRAS data to the optical by this formula. The agreement in shape is outstandingly good for all wavenumbers $k \gtrsim 0.06 h \text{Mpc}^{-1}$. Of particular interest is the inflection around $k = 0.1 h \text{Mpc}^{-1}$. This had been pointed out for optical galaxies by Baugh & Efstathiou (1993), and now appears to be confirmed by the IRAS data – which are derived from a more local volume than the deeper APM data. The power spectrum is of the form of an almost exact power law for $k > 0.15 h \text{Mpc}^{-1}$, but flattens quite abruptly for smaller wavenumbers. As discussed above, there is clear disagreement between the optical and scaled IRAS data for $k \lesssim 0.05 h \text{Mpc}^{-1}$; rather than being surprised by this, we should consider it remarkable that the data agree so well to scales this large. Real-space measurements obtained by deprojection will always be prone to systematic errors on large scales, where the true small spatial signal can easily become swamped in projection. To see which determination to believe (if either) we should turn to clustering measurements in redshift space.

2.3 Clustering in redshift space

There are two sets of large-scale power-spectrum data for optical galaxies: from the CfA2 survey (Vogeley et al. 1992) and the APM-Stromlo survey (Loveday et al. 1992). In the latter case, the power spectrum has been converted from cell-count variances as in PD94, but this agrees very well with the recent direct calculation by Tadros & Efstathiou (1996). For IRAS galaxies, separate determinations have

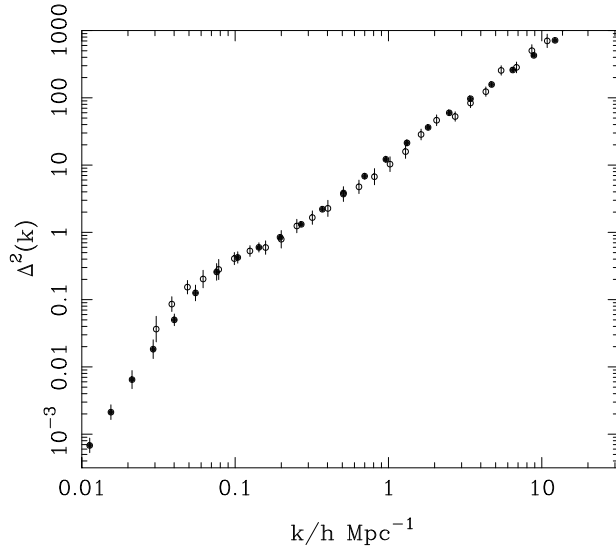


Figure 3. The real-space power spectrum of optical galaxies as estimated directly from the APM data of Fig. 1 (filled circles) and via a smoothly-varying scaling of the IRAS data from the same Figure. There is a good degree of unanimity concerning the inflection around $k \simeq 0.1 h \text{ Mpc}^{-1}$, but the two estimates diverge for $k \lesssim 0.06 h \text{ Mpc}^{-1}$.

been published by Fisher et al. (1993) and Feldman, Kaiser & Peacock (1994). However, it is probably better to use the result of Tadros & Efstathiou (1995), which combined the 1.2-Jy and QDOT datasets. Figures 4a and 4b compare these redshift-space power spectra with the real-space data from the previous Section, and different behaviour is immediately apparent. For optical galaxies, the redshift-space data lie above the real-space results at small k , but fall below them at large k . This is qualitatively the behaviour that would be expected: on large scales apparent 3D clustering is enhanced by coherent infall (Kaiser 1987), whereas on small scales it is reduced by the smearing of ‘fingers of God’ due to virialized random velocities. This trend is not really seen in IRAS galaxies; on small scales, the real-space power is the larger as expected, but on large scales the IRAS real-space measurements exceeds the redshift-space data by almost a factor of 2.

This is clear evidence that the largest-scale IRAS real-space data are too high; the three points with $k < 0.05 h \text{ Mpc}^{-1}$ will therefore be omitted from all subsequent analysis. For optical galaxies, Figure 4a suggests that the APM deprojection has worked extremely well out to the largest scale for which it is possible to compare with the shape of the redshift-space spectrum ($k \simeq 0.03 h \text{ Mpc}^{-1}$). The data considered by PD94 included other tracers on these scales, such as Abell clusters, which showed a large-scale slope consistent with the APM determination out to slightly larger scales ($k \simeq 0.02 h \text{ Mpc}^{-1}$), and the APM data appear to be reliable within their quoted errors up to this scale. Although results are given to smaller wavenumbers, we will take the conservative approach of not using them in the absence of independent verification. The conclusion of this comparison is therefore that the data shown in Figure 3 define the power spectrum of optical galaxy clustering to a precision of about 20 per cent over three decades in

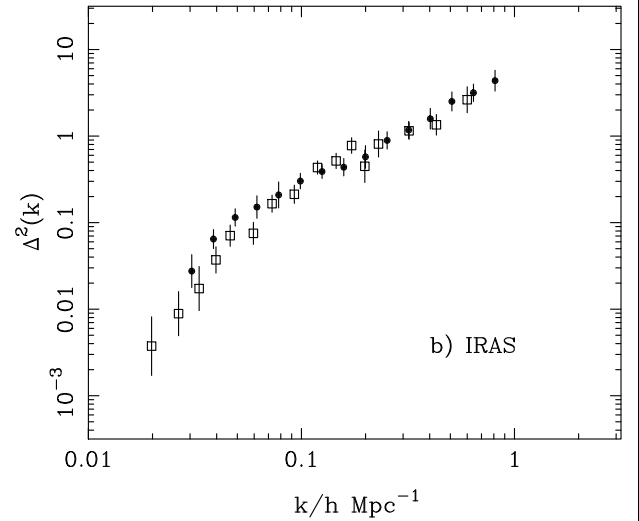
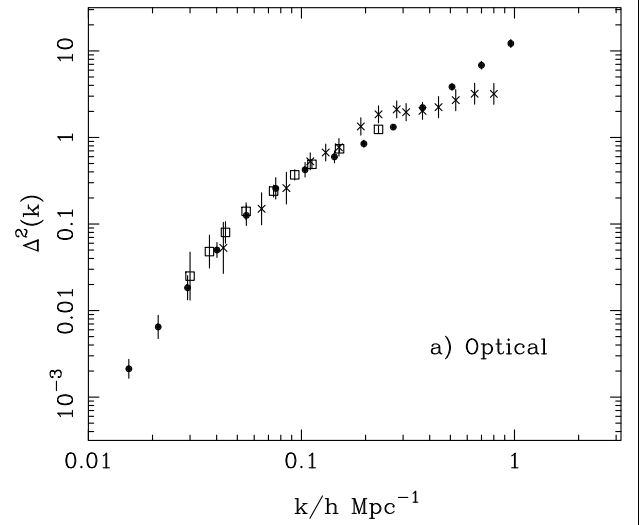


Figure 4. Comparison between the real-space power spectra of Fig. 1 and redshift-space data. The real-space data are shown as solid circles in both panels. Fig. 4a shows redshift-space results from the APM-Stromlo survey (open squares) and the CfA2 survey (crosses). Fig. 4b shows the redshift-space results from the combined 1.2-Jy and QDOT surveys as open squares. For optical galaxies, the redshift-space results are higher on large scales, as expected from peculiar-velocity distortions. The opposite is true for IRAS galaxies, suggesting that the largest-scale real-space points have been overestimated.

scale: $0.02 < k < 20 h \text{ Mpc}^{-1}$. With results of this verified accuracy now available, it should be possible to reach well-constrained conclusions about allowed models.

2.4 Redshift-space distortions

Before leaving this subject, it is interesting to look at the redshift-space distortions in a little more detail, since the size of the effect is sensitive to Ω . PD94 gave an analytical approximation for the distorting effects of peculiar velocities on power spectra, which expresses the power ratio as

a product of the large-scale Kaiser factor and a small-scale damping term:

$$\frac{P_{\text{redshift}}}{P_{\text{real}}} = [1 + \beta \mu^2]^2 D[k\mu\sigma_p]; \quad (11)$$

the power spectrum is anisotropic ($\mu = \hat{\mathbf{k}} \cdot \hat{\mathbf{r}}$), and this expression should be averaged over μ . The parameter describing the large-scale distortion is

$$\beta = \frac{\Omega^{0.6}}{b}; \quad (12)$$

the damping term depends on the assumed small-scale velocity distribution. For an exponential pair-wise distribution with pair-wise rms σ_p , the functional form is

$$D[k\mu\sigma_p] = [1 + (k\mu\sigma_p)^2/2]^{-1} \quad (13)$$

(Ballinger, Peacock & Heavens 1996). For describing the effect on the power spectrum, we need σ_p in length units rather than velocity (i.e. $\sigma_p \rightarrow \sigma_p/H_0$). From measurements of pairwise velocities, sensible values for σ_p will lie in the range $3 - 4 h^{-1}$ Mpc (Davis & Peebles 1983; Mo, Jing & Börner 1993; Fisher et al. 1994). The formula for the redshift-space power spectrum ignores quasi-linear modifications, and this assumption has been questioned by Fisher & Nusser (1996). However the above relation only amounts to a linear boost of power at small k , with a reduction in power at small scales that depends quadratically on k . If the expression is not pushed to too small scales, and if we are not too interested in the interpretation of the exact numerical size of the damping term, then this two-parameter formula should always be able to describe the data well.

Allowing the parameters β and σ_p to float, a maximum-likelihood fit can be performed between the real-space and redshift-space data (omitting the three largest-scale IRAS points). The real-space data, having smaller errors, are used to interpolate values at the k values of the redshift-space data, and the ratio is compared with the model. The resulting contours are shown in Figure 5. The optical results are far better constrained than the IRAS, reflecting the restricted range of k in the latter case, and there is a very clear preferred model:

$$\begin{aligned} \beta_{\text{opt}} &\simeq 0.40 \\ \sigma_p &\simeq 3.5 h^{-1} \text{ Mpc}. \end{aligned} \quad (14)$$

Note that the value of σ_p is very reasonable, despite the above caveats.

From the earlier discussion of relative bias, we would expect β for IRAS galaxies to be a factor 1.15 larger than the optical figure. If anything, the IRAS plot appears to favour smaller figures, but probably not too much confidence should be placed in this, because of the demonstrated problem with the large-scale real-space data. The worst points have been removed, but some residual systematics may remain in the retained points of largest scale, and these are the ones which give the main signal for β .

How seriously should the low value of β_{opt} be taken? A good reason for taking this analysis cautiously is that the statistical treatment of power-spectrum errors is rather simplistic. The published data points have been treated as independent, whereas it is inevitable that they will be correlated to some extent (Feldman et al. 1994); a more complete analysis would have to employ the full covariance ma-

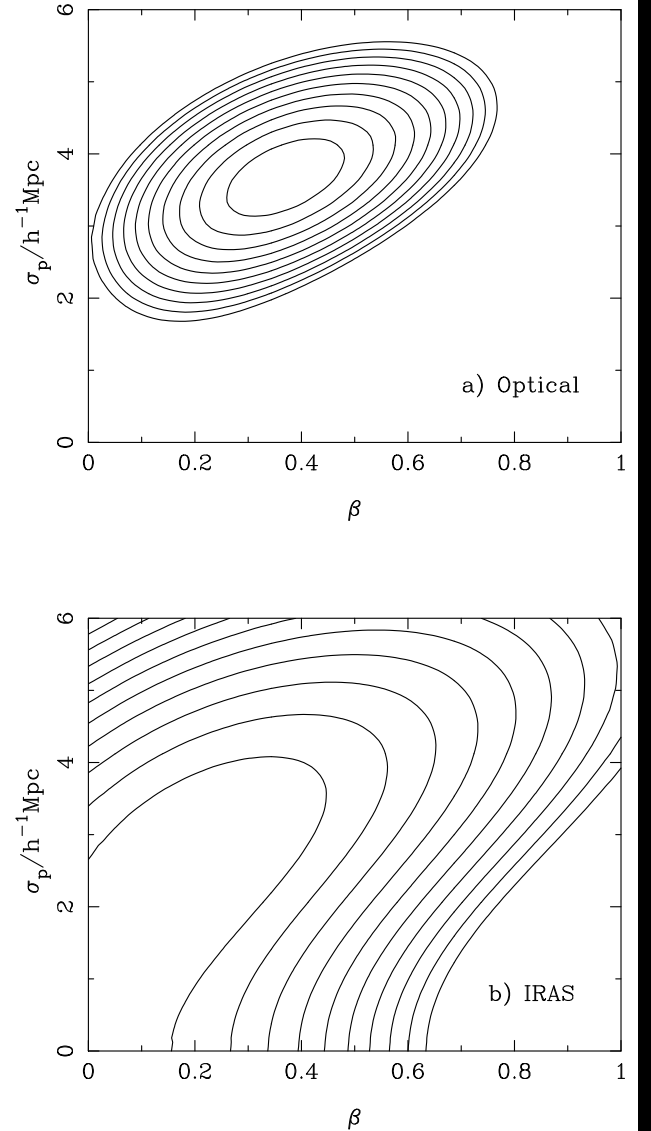


Figure 5. Likelihood contours (interval 0.5 in $\ln \mathcal{L}$) from fitting a model with large-scale Kaiser distortion plus finger-of-God damping to the data of Fig. 4. The parameter σ_p is the pairwise velocity dispersion of galaxies divided by H_0 , and thus expressed in units of h^{-1} Mpc. Fig. 5a shows the results for optical galaxies; Fig. 5b shows IRAS galaxies with the three largest-scale real-space points omitted. Note that $\beta_{\text{IRAS}} \simeq 1.15\beta_{\text{opt}}$ is expected. Even allowing for possible systematics in the analysis, it is very hard to see how $\beta = 1$ can be allowed.

trix. Nevertheless, the formal error in β_{opt} from this analysis is very small (about 0.05), and it is more likely that we should be worrying about systematics. The applicability of the Kaiser factor has been adequately tested in simulations, so the main concern is whether the amplitudes of either the real- or redshift-space data could be incorrect. The averaged linear boost from the Kaiser factor is

$$\frac{P_{\text{redshift}}}{P_{\text{real}}} = 1 + 2\beta/3 + \beta^2/5; \quad (15)$$

for $\beta = 1$ this is a factor 28/15 as against 1.30 for $\beta = 0.4$. $\beta = 1$ would therefore be allowed if the real-space power was

overestimated by a factor 1.43, or the redshift-space data too low by a similar amount. It is implausible that such a large factor can be found. The APM data were scaled by a factor of 1.25 to allow for the effects of evolution (see above). In detail, this number was obtained from a comparison with the amplitude of the real-space clustering in the APM-Stromlo redshift survey. Loveday et al. (1995) quote a scale-length of $r_0 = 5.1 \pm 0.2 h^{-1} \text{ Mpc}$, or an rms uncertainty in power of 7 per cent – much smaller than the error needed to allow $\beta = 1$. The other worry is that different surveys may sample galaxies of differing luminosities and thus obtain a variety of clustering signals. Indeed, Loveday et al. (1995) suggested that galaxies with $-19 < M_B < -15$ were clustered a factor roughly 2 more weakly on large scales than were more luminous galaxies. Is it possible that such an effect has reduced the amplitude of the optical redshift-space data? Certainly, the APM angular data refer to galaxies several magnitudes fainter than the redshift surveys. The real-space clustering signal therefore comes from a larger volume, but it is not likely to be due to galaxies of significantly different luminosities. Without applied redshift limits, the selection function of magnitude-limited galaxy surveys peaks for luminosities around L^* , and indeed the scaling tests for $w(\theta)$ as a function of depth applied by Maddox et al. (1990; 1996) leave little room for a depth-dependent effect. We therefore assume that the normalization uncertainty of 7 per cent in power is the principal contributor to the systematic error in β_{opt} . Added in quadrature to the statistical uncertainty, this gives the minimal error bar

$$\beta_{\text{opt}} = 0.40 \pm 0.12. \quad (16)$$

This uncertainty is approximately four times smaller than that obtained from a fuller analysis of the APM-Stromlo survey by Tadros & Efstathiou (1996), but it is not necessarily unrealistic. Tadros & Efstathiou considered $k \lesssim 0.1 h \text{ Mpc}^{-1}$ only, which increases the noise, and we have considered here both the APM-Stromlo and CfA2 surveys.

In any case, a figure of $\beta_{\text{opt}} \simeq 0.4$ is certainly consistent with a number of recent determinations from measurements of clustering anisotropy within a survey. Ratcliffe et al. (1996) find $\beta_{\text{opt}} = 0.55 \pm 0.12$ from the Durham/UKST survey, and Loveday et al. (1996) obtain $\beta_{\text{opt}} = 0.48 \pm 0.12$ from the APM/Stromlo survey. From the IRAS 1.2-Jy survey, Cole, Fisher & Weinberg (1995) obtain $\beta_{\text{IRAS}} = 0.52 \pm 0.13$. This convergence on a value of around $\beta = 0.5$ is in very serious disagreement with the values around unity inferred from the comparison of peculiar velocities with the galaxy density field (Dekel 1994), and it is of the greatest importance that the discrepancy be resolved. The impression from the present work is that $\beta = 1$ would require gross errors in clustering measurements, and it seems implausible that this can be the correct value. The lower values suggest that $\Omega \simeq 0.2 - 0.3$ if optical galaxies trace mass, or require $b \simeq 2$ in an Einstein-de Sitter universe.

3 NONLINEAR MASS POWER SPECTRA

3.1 Analytical method

In order to compare the clustering data with theoretical models, it is necessary to have an accurate means of predicting the effects of nonlinear growth on a given linear power

spectrum. This was made possible by the insight of Hamilton et al. (1991), who suggested a scaling formula for the growth of correlation functions. PD94 extended this method to work with power spectra and also to universes with $\Omega \neq 1$. The original suggestion of Hamilton et al. was that their scaling formula was spectrum independent, but Jain, Mo & White (1995) showed that this was not true. Peacock & Dodds (1996; PD96) give an improved version of the PD94 method which takes this into account, allowing the nonlinear spectrum that results from any smoothly-varying linear spectrum to be calculated. The method may be summarized as follows.

The nonlinear spectrum is a function of the linear spectrum at a smaller linear wavenumber:

$$\Delta_{\text{NL}}^2(k_{\text{NL}}) = f_{\text{NL}}[\Delta_{\text{L}}^2(k_{\text{L}})], \quad (17)$$

$$k_{\text{L}} = [1 + \Delta_{\text{NL}}^2(k_{\text{NL}})]^{-1/3} k_{\text{NL}}. \quad (18)$$

PD96 give the following fitting formula for the nonlinear function:

$$f_{\text{NL}}(x) = x \left[\frac{1 + B\beta x + [Ax]^{\alpha\beta}}{1 + ([Ax]^{\alpha} g^3(\Omega)/[Vx^{1/2}])^{\beta}} \right]^{1/\beta}. \quad (19)$$

In this expression, B describes a second-order deviation from linear growth; A and α parameterise the power-law which dominates the function in the quasilinear regime; V is the virialization parameter which gives the amplitude of the $f_{\text{NL}}(x) \propto x^{3/2}$ asymptote (where the behaviour enters the ‘stable clustering’ limit); β softens the transition between these regimes. The parameters and their dependence on spectrum are

$$A = 0.482 (1 + n/3)^{-0.947} \quad (20)$$

$$B = 0.226 (1 + n/3)^{-1.778} \quad (21)$$

$$\alpha = 3.310 (1 + n/3)^{-0.244} \quad (22)$$

$$\beta = 0.862 (1 + n/3)^{-0.287} \quad (23)$$

$$V = 11.55 (1 + n/3)^{-0.423}. \quad (24)$$

For linear spectra which are not a power-law, particularly the CDM model, PD96 suggested that a tangent spectral index as a function of linear wavenumber should be used:

$$n_{\text{eff}}(k_{\text{L}}) \equiv \frac{d \ln P}{d \ln k}(k = k_{\text{L}}/2). \quad (25)$$

The factor of 2 shift to smaller k is required because the tangent power-law at k_{L} overestimates (underestimates) the total degree of nonlinearity for curved spectra where n_{eff} decreases (increases) as k increases; the results are not greatly sensitive to the exact shift. This prescription is able to predict the nonlinear evolution of power-law and CDM spectra up to $\Delta^2 \simeq 10^3$ with an rms precision of about 7 per cent.

Note that the cosmological model is present in the fitting formula only through the growth factor g , which governs the amplitude of the virialized portion of the spectrum. According to Carroll, Press & Turner (1992), the growth factor may be approximated almost exactly by

$$g(\Omega) = \frac{5}{2} \Omega_{\text{m}} [\Omega_{\text{m}}^{4/7} - \Omega_{\text{v}} + (1 + \Omega_{\text{m}}/2)(1 + \Omega_{\text{v}}/70)]^{-1}, \quad (26)$$

where (m) and vacuum (v) contributions to the density parameter are distinguished; Ω without a subscript generally means Ω_m . When considering non-zero vacuum energy, it is usual to restrict attention to spatially flat models only. Models with $\Omega < 1$ thus come in two varieties: open ($\Omega_v = 0$) and flat ($\Omega_v = 1 - \Omega_m$).

3.2 CDM models and normalization of power spectra

As an illustration of these techniques in action, it is interesting to consider the CDM spectrum, which is a popular choice for the empirical description of the power spectrum, being a smoothly-curving form parameterised by a normalization σ_8 and a shape Γ^* . The CDM power spectrum is $\Delta^2(k) \propto k^{n+3} T_k^2$; usually $n = 1$ is adopted for the primordial spectrum. We shall use the BBKS approximation for the transfer function (which unfortunately suffered a misprint in PD94):

$$T_k = \frac{\ln(1 + 2.34q)}{2.34q} \times [1 + 3.89q + (16.1q)^2 + (5.46q)^3 + (6.71q)^4]^{-1/4}, \quad (27)$$

where $q \equiv (k/h \text{ Mpc}^{-1})/\Gamma^*$. The shape parameter Γ^* would be equal to Ωh in a model with zero baryon content. PD94 showed that there was a significant shift as a function of Ω_B , which was generalized to models with $\Omega \neq 1$ by Sugiyama (1995):

$$\Gamma^* = \Omega h \exp[-\Omega_B(1 + 1/\Omega)]. \quad (28)$$

Because of this scaling, $\Gamma^* = 0.94\Gamma$, where Γ is the shape parameter defined by Efstathiou, Bond & White (1992).

The normalization is specified by σ_8 : the linear-theory rms density contrast when averaged over spheres of radius $8 h^{-1} \text{ Mpc}$:

$$\sigma_R^2 = \int \Delta^2(k) \frac{dk}{k} \frac{9}{(kR)^6} [\sin kR - kR \cos kR]^2. \quad (29)$$

σ_R^2 is just $\Delta^2(k)$ at some effective wavenumber, which is very well fitted by

$$k_{\text{eff}}/h \text{ Mpc}^{-1} = 0.172 + 0.011[\ln(\Gamma^*/0.34)]^2. \quad (30)$$

What normalization is appropriate? A strong constraint comes from the abundance of massive clusters of galaxies, which is exponentially sensitive to the normalization, in a way that depends very little on spectrum. White, Efstathiou & Frenk (1993) argue that this gives

$$\sigma_8 = 0.57 \Omega^{-0.55}, \quad (31)$$

to a tolerance of roughly 10 per cent. They consider spatially flat models only, but the scaling for open models is likely to be very similar. Notice that the content of this equation is very similar to the effect of redshift-space distortions. The apparent (but non-linear) value of $b_{\text{opt}}\sigma_8$ is about 1, so the cluster constraint implies $\beta_{\text{opt}} \simeq 0.57$. This is a further reason for thinking that there must be a serious problem with the values of $\beta \simeq 1$ deduced from velocity-field studies. This also says that the cluster abundance constraint gives a very similar value for the normalization to that obtained from small-scale pairwise velocity dispersions, since they scale with Ω in almost the identical way. Taken literally,

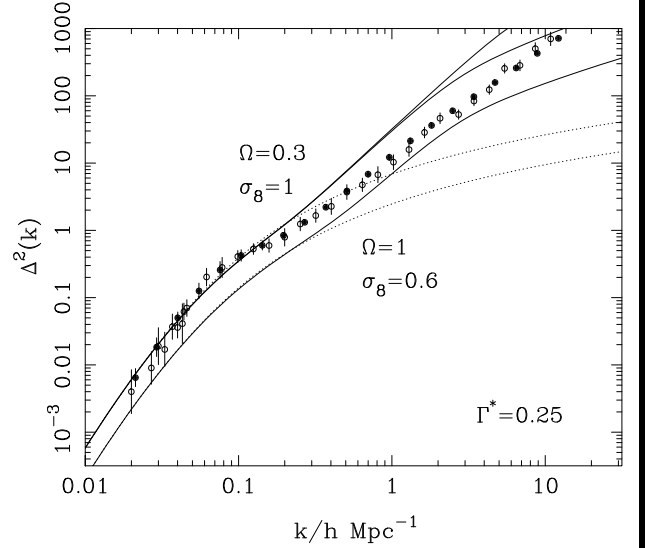


Figure 6. The optical-galaxy power spectrum of Fig. 3 with the discrepant scaled IRAS points omitted (APM data are shown as solid points, scaled IRAS data as open circles for $k > 0.05 h \text{ Mpc}^{-1}$). Also shown as open circles for smaller wavenumbers are the redshift-space data from Fig. 4, corrected assuming $\beta_{\text{opt}} = 0.4$, $\sigma_p = 3.5 h^{-1} \text{ Mpc}$. CDM models with $\Gamma^* = 0.25$ and $\sigma_8 = 0.6$ & 1 are shown. Linear spectra are shown dotted, with nonlinear spectra shown solid. For the lower normalization, $\Omega = 1$ is assumed; for the higher normalization, $\Omega = 0.3$ open and flat models are shown (open being the higher). The unbiased models greatly exceed the small-scale data; the $\Omega = 1$ model would require bias which was a strongly non-monotonic function of scale.

the White et al. normalization would imply that optically-selected galaxies are antibiased for $\Omega \lesssim 0.3$, whereas M/L ratios in clusters would prefer $\Omega \simeq 0.15 - 0.2$ in the absence of bias. We shall ignore this slight uncertainty and treat low-density models under the assumption that optically-selected galaxies trace mass as a first approximation: $\sigma_8 = 1$. For Einstein-de Sitter models, however, this assumption would make no sense and a lower normalization must be adopted; we take $\sigma_8 = 0.6$. Small variations on these assumptions do not change the conclusions.

Figure 6 shows the predictions of CDM models with these normalizations and the shape parameter $\Gamma^* = 0.25$ claimed by PD94 to fit the shape of large-scale structure very well. The Einstein-de Sitter model and $\Omega = 0.3$ models (open and flat) are shown, and none fare very well. As expected, the low-density models follow the low- k clustering data rather well, but both open and flat models start to predict too much small-scale power for $k \gtrsim 0.2 h \text{ Mpc}^{-1}$, and they do not produce much of an inflection around $k \simeq 0.1 h \text{ Mpc}^{-1}$. The open and flat models fare equally badly in this respect, only starting to part company at $k \gtrsim 1 h \text{ Mpc}^{-1}$. Changing Ω would only change the predicted spectrum in this regime, and so would not cure the problem. This tendency for low-density unbiased CDM models to overpredict the small-scale power was noted in the $\Gamma^* = 0.2$ case by Efstathiou, Sutherland & Maddox (1990), and recently rediscovered by Klypin et al. (1996). Because of its lower normalization, the $\Omega = 1$ model at least does not exceed the data, but it still presents serious problems. The

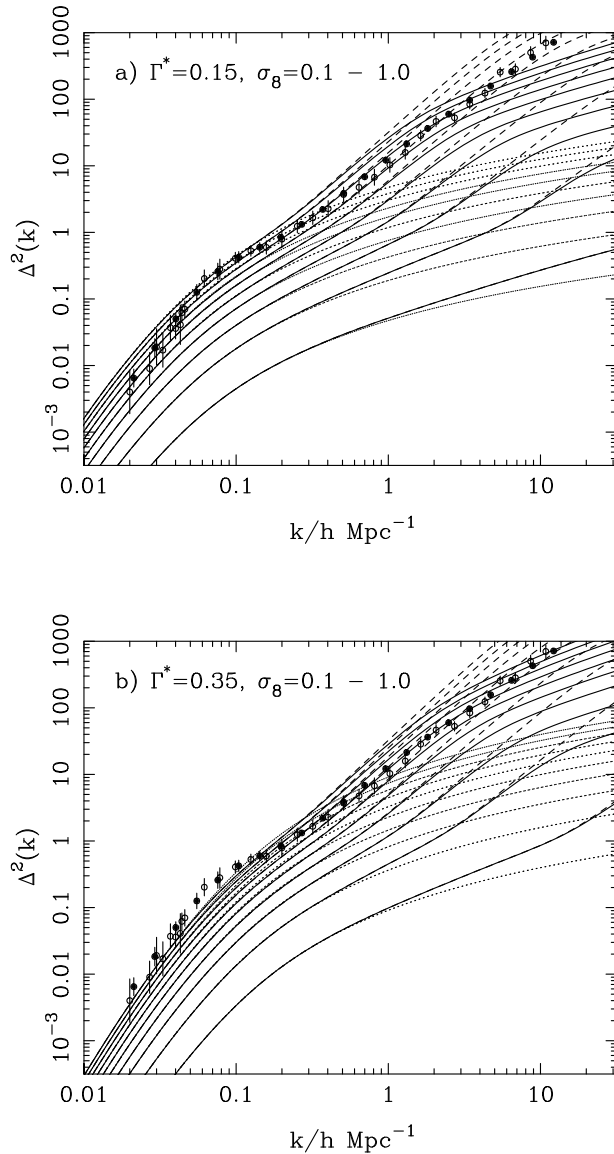


Figure 7. An extended form of Fig. 6, showing CDM spectra with a) $\Gamma^* = 0.15$, b) $\Gamma^* = 0.35$, for σ_8 values between 0.1 and 1, in steps of 0.1. Linear spectra are dotted; the solid lines show nonlinear spectra for $\Omega = 1$, and the dashed lines show an open $\Omega = 0.3$ model.

implied bias is an oscillating function of scale: it has a local maximum around $k \simeq 0.1 h \text{ Mpc}^{-1}$ (again, no inflection is predicted), and a local minimum around $k \simeq 3 h \text{ Mpc}^{-1}$. No local bias scheme could give this non-monotonic behaviour (Coles 1993).

These problems are general, and not specific to the exact value of Γ^* used, or the tilt adopted. For models with $n \neq 1$, the results over the range of k considered are indistinguishable from those with $n = 1$ and a different value of Γ^* . Figure 7 shows a grid of models with varying σ_8 for $\Gamma^* = 0.15$ and 0.35 , and they show that the same kind of problems persist:

- (1) Unbiased models with $\sigma_8 \simeq 1$ over-produce small-scale power. The correct level of power around $k = 1 h \text{ Mpc}^{-1}$ requires $\sigma_8 \simeq 0.7$, but the large-scale data are then very

badly fitted, whatever value of Γ^* is assumed.

- (2) No model reproduces the inflection seen around $k \simeq 0.1 h \text{ Mpc}^{-1}$.
- (3) Only open low-density models produce a small-scale power spectrum which resembles the observed power law. Both $\Omega = 1$ models and flat low-density models reach the stable clustering regime and turn to a flatter slope rather abruptly at $\Delta^2 \simeq 50 - 100$. These models need a bias scheme capable of generating a sharp kink at just the required point.

The reason PD94 were not able to reach these conclusions is because of the improved nonlinear treatment used here, which allows high accuracy in the predictions at $0.5 \lesssim k \lesssim 10 h \text{ Mpc}^{-1}$. PD94 considered only the deduced linear spectrum at $\lesssim 0.5 h \text{ Mpc}^{-1}$, which reduces the amplitude of the conflict between CDM models and observation. Comparison of nonlinear spectra is clearly the more sensitive test, given accurate nonlinear predictions; the nonlinear treatment of PD96 in fact gives a slightly larger response for low- Γ^* CDM models, which exacerbates the difficulties for CDM. The conclusion is therefore that the CDM spectrum is of the wrong shape, and cannot be made to fit the data, however its parameters are adjusted.

3.3 Empirical linear power spectra

What appears to be required is a linear spectrum which bends more abruptly around $k \simeq 0.1 h \text{ Mpc}^{-1}$, and the inflection at this point is therefore to be interpreted as a residual feature from the linear spectrum. The precise linear form can be recovered by running the nonlinear apparatus backwards, although this is now a more complicated procedure than in PD94, because the nonlinear response depends on the slope of the linear spectrum. We have to proceed iteratively, assuming an initial linear spectral slope, and then refining the dependence of this slope on scale.

For low-density models, it is reasonable to perform this linearization under the assumption that the clustering of optically-selected galaxies is not significantly biased. Models with $\Omega = 1$ present greater difficulties: there is no point in recovering a linear spectrum which would evolve into the observed clustering when we know that the resulting amplitude of mass fluctuations would be far too high. Before performing the linearization, we need to allow for bias, but this requires a specific hypothesis for the variation of bias with scale. Since we do not know what this variation is, the best that can be done is to illustrate how the linearized spectrum depends on different assumptions for the bias. The nonlinear response is by definition highly sensitive to the linear spectrum, so there is at least some hope that the recovered linear spectrum will not depend critically on assumptions about bias. We shall consider two examples. The simplest is a constant linear bias:

$$\Delta_{\text{opt}}^2 = b^2 \Delta_{\text{mass}}^2; \quad (32)$$

in the light of the earlier discussion, $b = 1.6$ is about the correct number. This is certainly an extreme example, since we have seen that bias generally increases at small scales. For an alternative model, we can take a hint from nature and guess that the scale dependence of the bias is similar to the form that relates optical galaxies and IRAS galaxies:

$$1 + \Delta_{\text{opt}}^2 = [1 + b_1 \Delta_{\text{mass}}^2]^{b_2} \quad (33)$$

Non-linear bias models of this type are considered in detail by Mann, Peacock & Heavens (1996). Their work shows that a broad range of biasing prescriptions yield a galaxy power spectrum with a relationship to the mass power spectrum which is well fitted by such a functional form. For IRAS/optical bias, we had $b_1 \simeq b_2$, and so this suggests $(b_1, b_2) = (1.6, 1.6)$, for an overall linear bias of 1.6. There is no guarantee that this is the exact bias that applies to the real universe, but it will suffice to illustrate the effects of a realistic amount of scale-dependent bias. Figure 8 shows the recovered linear spectra for these various cases.

In all cases, what we see is a spectrum which breaks rather abruptly, as expected from the discussion of the failures of the CDM spectrum. As hoped, the $\Omega = 1$ reconstructions with different bias assumptions differ only slightly. For $k \lesssim 1 h \text{ Mpc}^{-1}$, a satisfactory empirical description of the data is provided by a simple transition between two power laws:

$$\Delta^2(k) = \frac{(k/k_0)^\alpha}{[1 + (k/k_1)^{(\alpha-\beta)/\delta}]^\delta}, \quad (34)$$

as shown in Figure 9. For low-density unbiased models, the parameters are

$$\begin{aligned} k_0 &= 0.42 h \text{ Mpc}^{-1} \\ k_1 &= 0.057 h \text{ Mpc}^{-1} \\ \alpha &= 0.74 \\ \beta &= 4.0 \\ \delta &= 0.6. \end{aligned} \quad (35)$$

A value of $\beta = 4$ corresponds to a scale-invariant spectrum at large wavelengths, whereas the effective small-scale index is $n = -2.3$. Note that here and below we focus on $\Omega = 0.3$ as a representative low-density model, but almost indistinguishable linearized results would be obtained if this was varied by up to a factor 2 (unless bias was varied as a function of Ω). For $\Omega = 1$, the parameters change to

$$\begin{aligned} k_0 &= 5.0 h \text{ Mpc}^{-1} \\ k_1 &= 0.066 h \text{ Mpc}^{-1} \\ \alpha &= 0.42 \\ \beta &= 4.0 \\ \delta &= 1.0, \end{aligned} \quad (36)$$

independent of the assumed scale dependence of bias for linear wavenumbers $k \lesssim 0.4 h \text{ Mpc}^{-1}$. These fits are similar in form to a model advocated by Branchini, Guzzo & Valdarnini (1994). On the basis of a redshift survey of the Perseus-Pisces region, they suggested a phenomenological power spectrum in which the small-scale index was $n = -2.2$, with a break at $k \simeq 0.08 h \text{ Mpc}^{-1}$. They did not consider the nonlinear evolution of any alternative model, but this was an early indication that a very flat small-scale spectrum might fit the clustering data.

It should be noted that this linearization process is close to being unstable, because the nonlinear response rises very rapidly as the linear spectrum approaches $n = -3$. The small-scale index cannot greatly exceed $n = -2.3$, but it could be flatter. This is an issue for the low-density models in particular, as can be seen in Fig. 8a. The analytic fit is not perfect, with the data lying slightly higher around

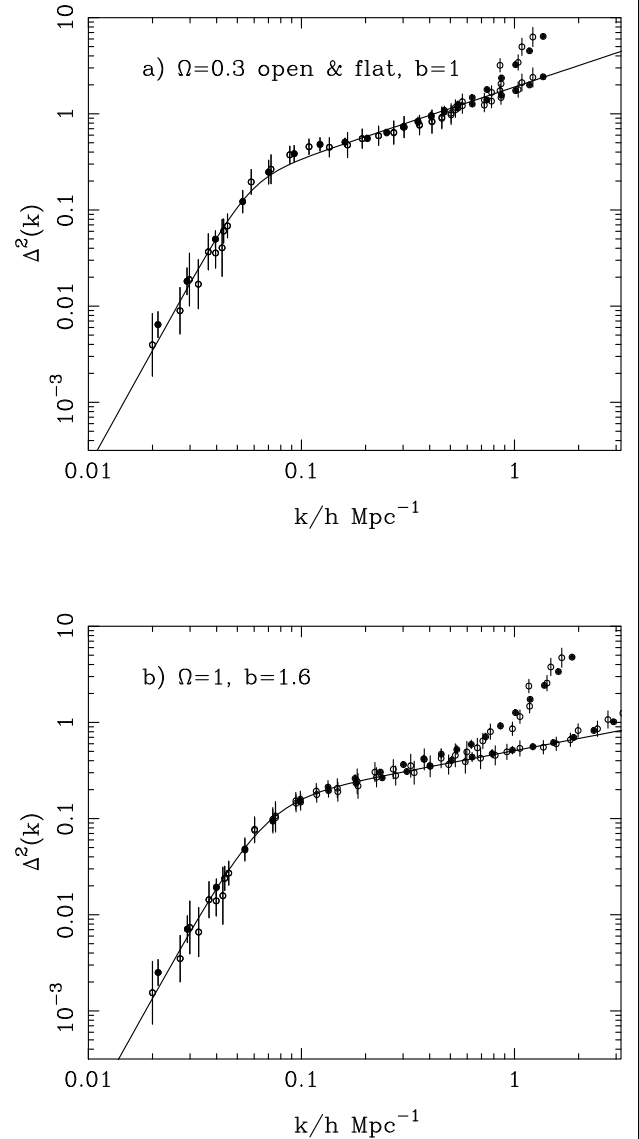


Figure 8. Linearized versions of the optical power-spectrum data from Fig. 3, with APM results shown as solid points and scaled IRAS results as open circles. The solid lines are the power-law fits described in the text. Fig. 8a assumes no bias and shows results for open and flat $\Omega = 0.3$ models. These are similar on large scales, but the flat results require an abrupt steepening on small scales. Fig. 8b assumes $\Omega = 1$ and a linear bias of $b = 1.6$. If this is independent of scale, a small-scale feature is again required. For the more plausible scale-dependent bias described in the text, the linear spectrum is more nearly a single power law on small scales.

$k = 0.1 h \text{ Mpc}^{-1}$ and lower around $k = 0.3 h \text{ Mpc}^{-1}$. It is not possible to achieve a better fit, since this would require a local $n \simeq -3$ between $k \simeq 0.1 h \text{ Mpc}^{-1}$ and $0.2 h \text{ Mpc}^{-1}$. Such a flat spectrum would suppress the required power at $k = 0.3 h \text{ Mpc}^{-1}$, resulting in a peak in the linear spectrum at $k \simeq 0.1 h \text{ Mpc}^{-1}$. This is a fascinating possibility, but needs further investigation; the PD96 formulae have not been tested in the regime where the concept of a hierarchical density field breaks down. In any case, the errors on the data are such that the apparent misfit in Fig. 8a is of

questionable significance. For the present, the conservative approach is to stick with a monotonically increasing $\Delta^2(k)$, and the linearization in Fig. 8a therefore assumes the local slope $n(k)$ given by the analytic fit.

The fits work well enough at large scales, but in most cases they fail to fit the reconstruction at the smallest scales, and there is generally a ‘bump’ where the power increases quite abruptly. This can be understood with reference to the nonlinear spectra shown in the discussion of the evolution of the CDM spectrum. High-density and flat models with $\Lambda \neq 0$ tend to hit the virialized regime quite early, flattening the predicted power spectra for $\Delta^2 \gtrsim 100$. This is not seen in the data, and so a feature must be introduced into the linearized spectra in order to keep the nonlinear spectrum steep. For open models, this feature is not required for $\Omega < 0.3$. For $\Omega = 0.3$, the small-scale flattening is just starting to become significant, and smaller values would arguably be preferred. However, as discussed below, the higher value gives a better match to the data on clustering evolution. The fitting formula is easily amended to deal with this small-scale behaviour:

$$\Delta^2(k) = \frac{(k/k_0)^\alpha + (k/k_2)^\gamma}{[1 + (k/k_1)^{(\alpha-\beta)/\delta}]^\delta}. \quad (37)$$

A value of $\gamma = 3$ ($n = 0$ spectrum) is appropriate, and the required normalization is $k_2 \simeq 0.72 h \text{ Mpc}^{-1}$ for the flat $\Omega = 0.3$ case (increasing to 0.79 for $\Omega = 0.2$), or $k_2 \simeq 0.91 h \text{ Mpc}^{-1}$ for $\Omega = 1$. The spatial scales of interest for the small-scale feature, where correlations in the range 100 – 1000 are found, are separations of about $0.5 - 0.2 h^{-1} \text{ Mpc}$.

The alternative explanation is that the mass spectrum does flatten on these scales, but bias steepens it again. This is hard to rule out, but it does seem a little contrived that the effects of bias and gravitational nonlinearity should conspire to cancel each other out in this way. The only case where such a conspiracy is not required is when the universe is open with $\Omega \lesssim 0.3$; the virialized regime then occurs at sufficiently high overdensity that the predicted nonlinear spectrum remains almost a single power law up to $\Delta^2 \gtrsim 1000$, without having to introduce a feature in the linear spectrum. This point is illustrated in Figure 9.

3.4 Physical models

What is the interpretation of the linear spectrum? We have argued that CDM models are inadequate for describing anything but the very large-scale portion of the spectrum, and so the temptation to put a physical meaning to the best-fitting shape parameter through $\Gamma^* \simeq \Omega h$ may not always be correct. Nevertheless, many of the alternative models produce less small-scale power than a CDM model of a given density, so a lower limit to Ωh may be obtained by this argument. In this case, it is worth noting that a substantial density is implied: $\Omega \leq 0.2$ would be difficult to reconcile with any reasonable Hubble constant.

Within the compass of models where the dark matter is still cold and collisionless, there is only one alternative in the literature that produces a spectrum with the required sharp break: isocurvature initial conditions (Efstathiou & Bond 1986). However, in this case the large-scale rms CMB anisotropies would be a factor of 6 higher for a given level of large-scale matter fluctuations, and so this possibility must

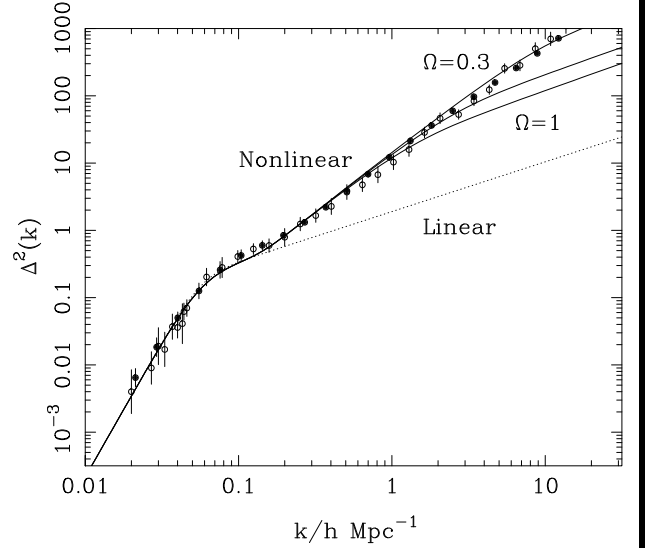


Figure 9. Illustrating the fit of the two power-law model for the linear spectrum in the case of an $\Omega = 0.3$ open model. For the same linear spectrum, $\Omega = 0.3$ flat and $\Omega = 1$ models produce successively more marked flattening of the small-scale nonlinear spectrum. In these latter cases, a small-scale feature in the linear spectrum is required in order to keep the nonlinear spectrum steep.

Table 1. Best-fitting parameters for physical power spectra.

Model	Ω	Γ^*	f_ν
CDM	1	0.109	0
CDM	0.3	0.090	0
HDM	1	0.440	1
HDM	0.3	0.429	1
MDM	1	0.373	0.307
MDM	0.3	0.393	0.335

be rejected.

Assuming that ‘designer inflation’ and features in the primordial spectrum are rejected, we are left with the alternative of modifying the matter content. Interesting possibilities with high density are either mixed dark matter (e.g. Holtzman 1989; Taylor & Rowan-Robinson 1992; Klypin *et al.* 1993), or non-Gaussian pictures such as cosmic strings + HDM, where the lack of a detailed prediction for the power spectrum helps ensure that the model is not yet excluded (Albrecht & Stebbins 1992). It has been argued that an MDM spectrum with $\Omega h \simeq 0.5$ and approximately 30 per cent of the density in a hot component gives a spectral shape quite close to the empirical one. This would be true whether or not the total density was $\Omega = 1$, so one could also consider low-density MDM models. Pogosyan & Starobinsky (1995) give analytic formulae for the MDM transfer function, which they express as $T_{\text{MDM}} = T_{\text{CDM}}(k, h)D(k, h, \Omega_\nu)$, assuming $\Omega = 1$. If we remove this assumption, then the formulae can still be used, replacing k/h^2 by $[k/h]/\Gamma^*$ and Ω_ν by $f_\nu = \Omega_\nu/\Omega$. Note that there appears to be a misprint in the definition of the parameter β after their equation (3): it should be $\beta = [5 - (25 - 24\Omega_\nu)^{1/2}]/4$.

Fig. 10 shows the fit of this 2-parameter form to the linear power data, and contrasts this with the poor fit of CDM alone. This plot also compares pure HDM models, restricting

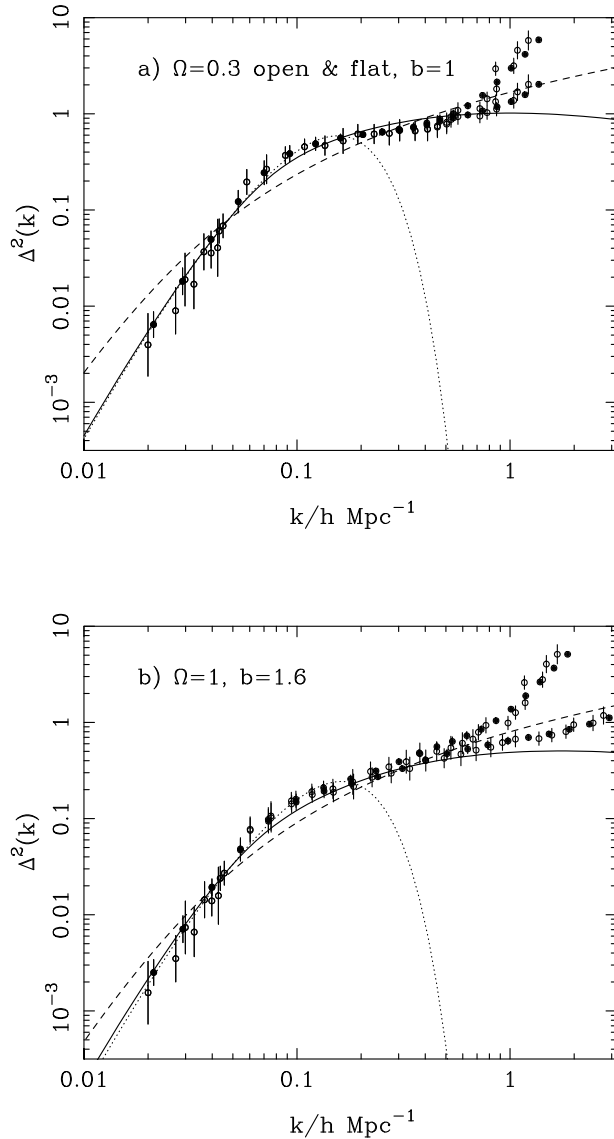


Figure 10. The linearized spectrum data from Fig. 8, fitted with CDM (dashed), HDM (dotted) and MDM (solid) models. The best-fitting parameters are given in Table 1. MDM spectra provide the best fit, although HDM works well over the range to which the fit was restricted ($k < 0.2 h \text{ Mpc}^{-1}$ for HDM; $k < 1 h \text{ Mpc}^{-1}$ in the other cases).

the fit to the large-scale portion of the spectrum. Both HDM and MDM achieve a satisfactory fit for $k \lesssim 0.2 h \text{ Mpc}^{-1}$, and both spectra in fact make similar nonlinear predictions, underlining the earlier discussion on the instability of the linearization at large k . The parameters for these models are given in Table 1. The preferred values of Γ^* for HDM and MDM are something of a puzzle, since they are in the region of 0.4. This is too large to be consistent with low-density models for any reasonable Hubble constant, and would require $h \simeq 0.4$ for $\Omega = 1$. Many would also think that this is an unreasonable number, but it does at least yield a reasonable age for $\Omega = 1$ models. The Einstein-de Sitter universe is thus the only case where a consistent picture for the present universe can be made using an *a priori* physical model for

the power spectrum.

However, both HDM and MDM models face problems that are generic to any model with a very flat high- k spectrum in a high- Ω universe: difficulty in forming high-redshift objects. These are classic problems for HDM models, but also appear to be fatal for MDM (Mo & Miralda-Escudé 1995; Ma & Bertschinger 1994; Mo & Fukugita 1996). As shown above, high-density models also have difficulty in achieving a steep correlation function on small scales; both this point and high- z galaxy abundances argue for an additional small-scale component in the linear spectrum, if $\Omega = 1$. Both these difficulties disappear in an open universe, but it is hard to feel much enthusiasm for the ugly combination of MDM and $\Omega < 1$. Apart from aesthetics, we have seen that the value of Γ^* in this model is much higher than would be required in a universe with reasonable h and $\Omega \simeq 0.3$. In summary, all known physically-motivated models for the clustering power spectrum face very serious difficulties. It appears that some completely new alternative is needed.

4 EVOLUTION OF CLUSTERING

Having identified a variety of routes by which the present-day clustering of galaxies could have arisen, the obvious way to break the degeneracy is to look at the change of clustering with epoch, for which the various models make quite different predictions. For a number of years, the evolution of clustering has been probed by means of the angular correlation function, $w(\theta)$, and its change with magnitude limit. Limber's equation (e.g. Peebles 1980) allows a relation to be made between $w(\theta)$ and $\xi(r)$ once the redshift distribution is known for the galaxies under study. A number of studies have been carried out, of which some of the more recent are Efsthathiou et al (1991); Neuschaefer, Windhorst & Dressler 1991; Couch, Boyle & Jurcevic (1993); Roche et al. (1993). Although there has been some debate over the interpretation of these studies owing to the uncertain redshift distribution at very faint limits, there has been a measure of agreement over two conclusions:

- (1) The slope of the correlation function appears not to alter with redshift. If $\xi(r) \propto r^{-\gamma}$, then γ is in the region of 1.7 at all redshifts up to $z \simeq 1$.
- (2) The rate of evolution of clustering is relatively rapid, close to the linear-theory rate of evolution in an Einstein-de Sitter universe: $\xi(r, z) \propto (1+z)^{-2}$.

4.1 The predicted rate of evolution

Several workers have commented that these conclusions are paradoxical. A common model for predicting the evolution of clustering is Peebles' stable-clustering argument. In the limit that clusters are virialized entities of fixed proper size, clustering will change with epoch only because the background density evolves as $(1+z)^3$. In proper length units, this predicts $\xi(r_p, z) \propto (1+z)^{-3}$. In comoving units, used everywhere else, one is then led to write

$$\xi(r, z) = [r/r_0]^{-\gamma} (1+z)^{-(3-\gamma+\epsilon)}, \quad (38)$$

where $\epsilon = 0$ is stable clustering; $\epsilon = \gamma - 3$ is constant comoving clustering; $\epsilon = \gamma - 1$ is $\Omega = 1$ linear-theory evolution.

It is usually argued that biased CDM-like universes would therefore predict ϵ significantly less than zero, whereas the data favour $\epsilon \simeq 1$. An alternative way of looking at this is to ask how the typical proper size of a cluster changes with redshift: $R_p \propto (1+z)^{-\beta}$. Clearly, $\epsilon = (\gamma - 3)\beta$ and so $\epsilon \sim 1$ implies that $\beta \sim -1$: clusters must contract about as fast as the universe expands.

In short, the paradox is that galaxy clustering is required to evolve in a way that resembles linear theory in an $\Omega = 1$ universe, keeping the same shape and changing its amplitude rapidly, even though the data are well into the non-linear regime. Since the above analysis says that clustering should then evolve more slowly, this has led some (e.g. Efsthathiou et al. 1991) to suggest that the galaxies seen in the faint surveys are a different population, with much weaker intrinsic clustering.

However, there is a serious loophole in the stable-clustering argument, since we have seen that the observations of clustering mainly do not reach the stable-clustering regime. In the intermediate quasilinear transition to linear behaviour, PD96 have shown that the steep form of f_{NL} produces evolution of clustering that is much more rapid:

$$\xi(r, z) = [r/r_0]^{-\gamma} [D(z)]^{(6-2\gamma)(1+\alpha)/3}, \quad (39)$$

where $\alpha \simeq 3.5 - 4.5$ is the transition slope in f_{NL} and $D(z)$ is the linear-theory density growth rate ($D(z) = (1+z)^{-1}$ if $\Omega = 1$). For $\alpha = 4$, $\gamma = 1.7$, this gives $\xi \propto D^{4.3}$, which is about twice the observed evolution if $\Omega = 1$. Ironically, we still conclude that the observed clustering evolution is inconsistent with nonlinear evolution in an $\Omega = 1$ universe – but now because the real evolution is too slow, not too fast. Agreement with the data requires a linear growth rate which is about half as rapid as the $\Omega = 1$ $D(z) \propto (1+z)^{-1}$. Figure 11 shows the linear-theory growth factor plotted against scale factor for various values of Ω for open and flat models (see e.g. Carroll et al. 1991). This suggests that the observed rate of evolution can be supplied naturally by $\Omega \simeq 0.2 - 0.3$ [open] or $0.1 - 0.2$ [flat], without having to postulate that the faint galaxies are a separate population.

We can do better than this general discussion by looking at the detailed data on the evolution of clustering from the Canada-France Redshift Survey (Le Fèvre et al. 1996). From a sample of 591 galaxies selected to $I \lesssim 22.5$, the CFRS team are able to deduce the spatial clustering in several redshift bands out to $z = 1$. They avoid redshift-space effects by working with the projected correlation function discussed in the context of IRAS galaxies. Le Fèvre et al. call this quantity $w(r_p)$, but we shall use the symbol $\Xi(r)$ as before. The only important difference is that Le Fèvre et al. quote their results as a function of proper separation, whereas comoving units are preferred here. It will also be more convenient to use the dimensionless function $\Xi(r)/r$, which is then directly related to overdensity and so does not change as the length units are scaled from proper to comoving.

The other technicality to worry about is that the deduced values of $\Xi(r)/r$ depend on the cosmological model used. The CFRS results are quoted for $\Omega = 1$; inspection of the integral relating Ξ to ξ says that the projected results

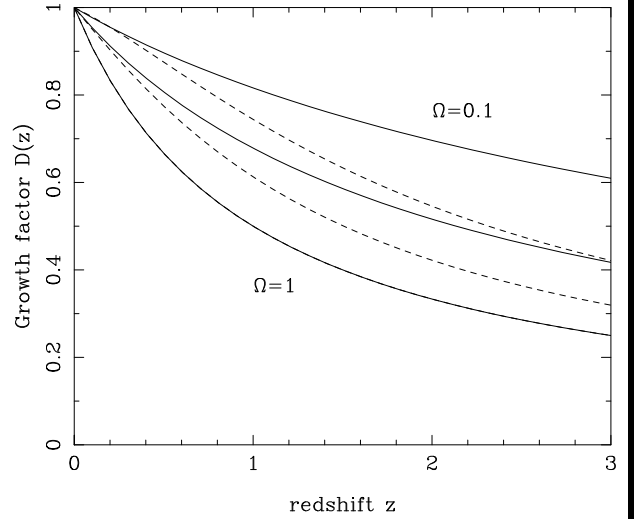


Figure 11. The linear growth in density perturbations, scaled to unity at the present, for $\Omega = 1, 0.3$ & 0.1 . Open models are shown as solid lines, flat models are dashed.

must scale in the following way for other cosmologies:

$$\frac{\Xi_1(r_1)}{r_1} = \frac{d\chi_1}{d\chi_\Omega} \frac{D_\Omega}{D_1} \frac{\Xi_\Omega(r_\Omega)}{r_\Omega}, \quad (40)$$

where the increment of comoving distance is

$$R_0 d\chi = \frac{[c/H_0] dz}{\sqrt{\Omega_v + \Omega_m(1+z)^3 + (1 - \Omega_m - \Omega_v)(1+z)^2}}, \quad (41)$$

$D = R_0 S_k(\chi)$ is comoving angular-diameter distance, and $R_0 = (c/H_0)|1 - \Omega_m - \Omega_v|^{-1/2}$. At a given r , Ξ/r also depends on cosmology because $r_1/r_\Omega = D_1/D_\Omega$. Overall, this shift and the multiplicative factors cause a larger Ξ/r to be inferred for low Ω . Assuming a slope of 1.65, the total shift of power at $z = 1$ is a factor 1.4 ($\Omega = 0.3$ open) or 1.9 ($\Omega = 0.3$ flat); these models require an evolutionary ϵ which is smaller by 0.5 and 0.9 respectively. There is thus something of a cosmic conspiracy: the low-density models in which dynamics yields less rapid clustering evolution are also those in which geometry causes less rapid evolution to be inferred from a given set of data.

4.2 Comparison of models and CFRS data

The results of a comparison between the CFRS data and various models are shown in Fig. 12. This shows that the projected correlations are very close to a single power law on all nonlinear scales, and that the amplitude changes by only a factor $\simeq 2$ between $z = 0.34$ and $z = 0.86$. The solid lines in Fig. 12 are the predictions of the double power-law spectra deduced from the local data, and they show that it is not easy to satisfy the twin constraints of the right shape and the right rate of evolution. All models tend to flatten on small scales as clustering reaches the virialized regime. For $\Omega = 0.3$ (open), this tendency is relatively minor, but for flat models it is a stronger effect, and produces a huge discrepancy in the case of $\Omega = 1$. If we are to live in an $\Omega = 1$ universe, then the two powers of ten discrepancy in small-scale clustering at high redshift revealed by Fig. 12c must be bridged by bias.

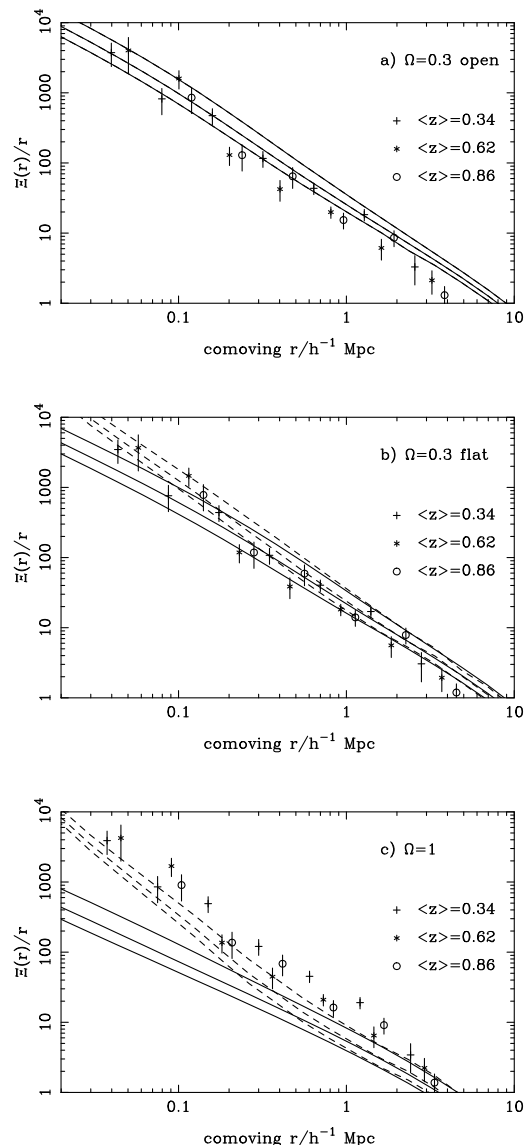


Figure 12. The CFRS projected clustering data (calculated as a function of comoving separation for three cosmologies) in three redshift ranges, compared to model predictions. The solid lines show the evolution predicted for the double power-law fits to the linear power spectra shown in Fig. 8. The dashed lines show the effect of adding an additional small-scale component to the linear spectrum, such as is needed to account for the present-day clustering spectrum on the smallest scales. In the case of the $\Omega = 1$ model, $b = 1.6$ at the present was assumed in order to obtain the mass spectrum. However, unless there is an additional small-scale component, the implied small-scale bias at high redshifts is very much greater than this, on scales where the spectrum is only mildly nonlinear.

This is implausible, not just because of the large amplitude of the bias, but because of the scale on which it occurs. If we ask what power spectrum is required to produce the observed power-law clustering, and compare it with the $\Omega = 1$ nonlinear prediction at $z = 0.86$, there is a discrepancy of a factor ~ 100 at the point where the prediction has $\Delta^2 \sim 1$. This conflicts with the general idea that local bias schemes would yield a near-constant bias where the mass

fluctuations are in the linear regime. If bias of this magnitude were a reality, it would mean that the galaxy distribution at high redshifts is dominated by non-local effects which bear little relation to the mass distribution. The known existence of massive high-redshift clusters (Luppino & Gioia 1995) is probably sufficient to rule out this idea.

Alternatively, we may take seriously the small-scale ‘kick-up’ in the linear spectrum that is required if the idea of strongly scale-dependent bias is rejected. The dashed lines in Fig. 12 show the results of adding in this feature, which changes the picture so that the variation between different cosmologies is now much reduced. The hypothetical additional component dominates the clustering in the $\Omega = 1$ case, and greatly increases the small-scale clustering in the Λ -dominated universe. We now see the standard stable-clustering evolution on most scales, with something more rapid on the largest scales. The stable-clustering rate in the Λ -dominated case is in reasonable accord with the data as calculated for this model, as expected from the above discussion. The same would also be true of the $\Omega = 1$ model if the same degree of bias ($b = 1.6$) applied at $z = 1$ as at $z = 0$. However, the model that comes closest to matching the overall shape and normalization of high-redshift clustering is the open universe. The main difficulty for this model is that it over-predicts the clustering at $z = 0.34$, as does the flat model. Le Fèvre et al. point out that the galaxies in this bin are of low luminosity only, so this may not be a problem. The highest-redshift bin contains the galaxies most nearly comparable to the local samples, and this is well matched in amplitude if $\Omega \simeq 0.3$. The preferred range for Ω depends on how seriously the CFRS errors are taken, but models outside the range $\Omega = 0.2 - 0.5$ give a poor fit if we stick to the assumption that there is little bias.

Given the realistic uncertainties in the clustering data, there is not much to choose between these latter alternatives. Le Fèvre et al. find a difference in clustering amplitude of a factor 1.8 between their red and blue sub-samples at intermediate redshifts, and the difference between models is of this order. One way of progressing from this point will be via data at higher redshifts, where the evolution of the different alternatives continues to diverge. Fernández-Soto et al. (1996) have argued from clustering of quasar absorption-lines that the scale-length for the correlation function at $z = 2.6$ is $r_0 \simeq 0.4 h^{-1} \text{ Mpc}$ (for $\Omega = 1$). The models with additional small-scale features in the linear spectrum would predict a much larger number, since evolution would have to proceed at the stable-clustering rate. If we could be convinced that the absorbers are not strongly antibiased, this result would therefore argue in favour of open models.

To sum up the conclusions of this Section, open universes with a linear spectrum in the form of a simple break between two power laws predict the correct form and rate of evolution of galaxy clustering up to $z = 1$. To obtain competitive results in $\Omega = 1$ or flat universes, we must believe that the linear power spectrum contains an extra feature, which comes to dominate for $k \gtrsim 1 h \text{ Mpc}^{-1}$.

5 CMB ANISOTROPIES

A consistent model must match the normalization of the mass fluctuations on large scales inferred from fluctuations

in the Cosmic Microwave Background. In making this comparison, it is important to be clear that the CMB fluctuations depend only on the very large-scale $P \propto k^n$ portion of the spectrum. Predictions of smaller-scale fluctuations such as the amplitude σ_8 then need additional information in the form of the transfer function. Rather than quoting the σ_8 implied by the CMB, it is therefore clearer to give the large-scale normalization separately.

The large-scale normalization from the 2-year COBE data in the context of CDM-like models is discussed by Bunn, Scott & White (1995); White & Bunn (1995); and Stompor, Górski & Banday (1995). The final 4-year COBE data favour slightly lower results (Bennett et al. 1996), and we scale to these in what follows. For scale-invariant spectra and $\Omega = 1$, the best normalization of the primordial spectrum is

$$\Delta^2(k) = (k/0.0737 \text{ h Mpc}^{-1})^4, \quad (42)$$

equivalent to $Q_{\text{rms}} = 18.0 \mu\text{K}$, or $\epsilon = 3.07 \times 10^{-5}$ in the notation of Peacock (1991), with an rms error in density fluctuation of 8%. For low-density models, a naive analysis as in PD94 suggests that the power spectrum should depend on Ω and the growth factor g as $P \propto g^2/\Omega^2$. Because of time dependence of gravitational potential (integrated Sachs-Wolfe effect) and spatial curvature, this expression is not exact, although it captures the main effect. From the data of White & Bunn (1995), a better approximation is

$$\Delta^2(k) \propto \frac{g^2}{\Omega^2} g^{0.7}. \quad (43)$$

This applies for low- Ω models both with and without vacuum energy, with a maximum error of 2% in density fluctuation provided $\Omega \geq 0.2$ (and gives the same σ_8 values as Górski et al. (1995), when the appropriate Γ^* corrections are made, to within 3%). Since rough power-law approximations for g are $g \simeq \Omega^{0.65}$ and $\Omega^{0.23}$ for open and flat models respectively, we see that the implied density fluctuation amplitude scales approximately as $\Omega^{-0.12}$ and $\Omega^{-0.69}$ for these two cases. The dependence is very weak for open models, but vacuum energy implies very much larger fluctuations. Note that these conclusions can be reached without being specific about the generation of anisotropies in open models. The existence of a curvature scale destroys the possibility of a unique scale-invariant spectrum, but such a concept does have a meaning on smaller scales. Since the main COBE signal comes from multipoles with $\ell \gtrsim 10$, the ambiguity in the predicted power from very low ℓ is unimportant unless $\Omega \lesssim 0.1$.

To avoid large uncertainties caused by different transfer functions, it is interesting to compare this COBE normalization with the observed power on the largest reliable scales:

$$\Delta_{\text{opt}}^2(k = 0.02 \text{ h Mpc}^{-1}) \simeq 0.005. \quad (44)$$

For this scale, the COBE scale-invariant prediction is 0.0054. Reducing Ω boosts this by a factor of 1.3 (open $\Omega = 0.3$) or 5.3 (flat $\Omega = 0.3$). The open number is well consistent with the observations, given the uncertainty in the transfer function at this point; the $\Omega = 1$ number is about three times too high (because the optical power should be roughly 1.6^2 times that of the mass in the $\Omega = 1$ case); the flat number is too high by at least a factor 6. The last two cases would therefore require a tilted spectrum.

According to the simplified analysis of PD94, COBE determines the spatial power spectrum at an effective wavenumber of $0.0012 \Omega^\delta \text{ h Mpc}^{-1}$, where $\delta = 1$ for open models, 0.4 for flat. The tilt needed to match the power at $k = 0.02 \text{ h Mpc}^{-1}$ is then $n = 0.64$ for $\Omega = 1$, or $n = 0.48$ for the flat $\Omega = 0.3$ case. If gravity waves are included with the usual inflationary coupling between wave amplitude and tilt, the effect is approximately

$$\Delta^2 \propto [1 + 6(1 - n)]^{-1} \quad (45)$$

Allowing for gravity waves therefore changes the required tilt to $n = 0.85$ ($\Omega = 1$) or $n = 0.75$ ($\Omega = 0.3$ flat), but the conclusion remains that low-density flat models need an extremely large degree of tilt in order to be viable. An open model therefore gives the most straightforward match between COBE and large-scale structure. It is interesting to note that Ratra et al. (1996) and Górski et al. (1996) also claim that the degree-scale anisotropy data are best fitted by an open model with $\Omega = 0.3 - 0.4$.

6 DISCUSSION

This paper has argued that the state of observations in galaxy clustering is now one of very high precision, both in the local power spectrum and in its evolution. Comparing this body of data with the predictions of nonlinear gravitational instability has yielded a number of general conclusions:

- (1) There is some evidence that more power is measured in redshift space than in real space, but not by as large a factor as expected for $\beta = 1$. A value $\beta \simeq 0.5$ is more consistent with the value of σ_8 inferred from the cluster abundance.
- (2) The shape of the power spectrum is not consistent with nonlinear evolution of any CDM-like model. The linear spectrum must have a sharp break around $k \simeq 0.1 \text{ h Mpc}^{-1}$.
- (3) Only low-density open models give a small-scale spectrum which is a power law. For other models, either a feature in the linear spectrum or an abrupt increase in small-scale bias is needed.
- (4) Open models with $\Omega \simeq 0.3$ also naturally give a spectrum which evolves at the observed rate while maintaining the same power-law shape. Such models are furthermore the only alternatives that are consistent with CMB anisotropies without requiring a large tilt.

These conclusions have been reached without invoking a specific mechanism for how galaxies trace mass. For low-density universes, we have been content to use M/L arguments to infer that the empirical degree of bias today is probably small, whereas substantial bias must exist if $\Omega = 1$. A more complete picture would have to be able to calculate the amount of bias and how it changes with redshift, but this is not well constrained at present. For example, Efstathiou (1995) showed how faint-galaxy clustering of the required amplitude could exist at $z = 1$ in an $\Omega = 1$ CDM universe by explicitly following the formation of low-mass haloes of dark matter in a numerical simulation, and identifying these with galaxies at that time. The problem with this argument is that different choices of halo mass (and halo environment) produce huge variations in the clustering amplitude, so this

route does not yet give a robust prediction for the clustering of faint galaxies. This ability to obtain very different clustering properties from different plausible ideas for how and where galaxies form warns us to take great care in interpreting clustering data; even so, it is undeniably striking how closely an open universe in which galaxies nearly trace mass accounts for a variety of aspects of galaxy clustering and its evolution.

ACKNOWLEDGEMENTS

Thanks are due to Carlton Baugh and Helen Tadros for communicating APM power-spectrum data, and to Will Saunders for illuminating conversations on the relation between optical and IRAS clustering.

REFERENCES

- Albrecht A., Stebbins A., 1992, *Phys. Rev. Lett.*, 69, 2615
Ballinger W.E., Peacock J.A., Heavens A.F., 1996, *MNRAS*, in press
Baugh C.M., Efstathiou G., 1993, *MNRAS*, 265, 145
Baugh C.M., Efstathiou G., 1994, *MNRAS*, 267, 323
Bennett C.L. et al., 1996, *ApJ*, 464, L1
Branchini E., Guzzo L., Valdarnini R., 1994, *ApJ*, 424, L5
Bunn E.F., Scott D., White M., 1995, *ApJ*, 441, 9
Carroll S.M., Press W.H., Turner E.L., 1992, *ARA&A*, 30, 499
Cole S., Fisher K.B., Weinberg D.H., 1995, *MNRAS*, 275, 515
Coles P., 1993, *MNRAS*, 262, 1065
Couch W.J., Jurcevic J.S., Boyle B.J., 1993, *MNRAS*, 260, 241
Davis M., Peebles P.J.E., 1983 *ApJ*, 267, 465
Dekel, A., 1994, *ARA&A*, 32, 371
de Lapparent V., Geller M.J., Huchra J.P., 1986, *ApJ*, 302, L1
Efstathiou G., Bond J.R., 1986, *MNRAS*, 218, 103
Efstathiou G., Bernstein G., Katz N., Tyson T., Guhathakurta P., 1991, *ApJ*, 380, 47
Efstathiou G., Bond J.R., White S.D.M., 1992, *MNRAS*, 258, 1P
Efstathiou G., Sutherland W.J., Maddox S.J., 1990, *Nat*, 348, 705
Efstathiou G., 1995, *MNRAS*, 272, L25
Feldman H.A., Kaiser N., Peacock J.A., 1994, *ApJ*, 426, 23
Fernández-Soto A., Lanzetta K.M., Barcons X., Carswell R.F., Webb J.K., Yahil, A., 1995, *ApJ*, 460, L85
Fisher K.B., Davis M., Strauss M.A., Yahil A., Huchra J.P., 1993, *ApJ*, 402, 42
Fisher K.B., Davis M., Strauss M.A., Yahil A., Huchra J.P., 1994, *MNRAS*, 267, 927
Fisher K.B., Nusser A., 1996, *MNRAS*, 279, L1
Górski K.M., Ratra B., Sugiyama N., Banday A.J., 1995, *ApJ*, 444, L65
Górski K.M., Ratra B., Stompor R., Sugiyama N., Banday A.J., 1996, *astro-ph/9608054*
Hamilton A.J.S., Kumar P., Lu E., Matthews A., 1991, *ApJ*, 374, L1
Holtzman J.A., 1989, *ApJS*, 71, 1
Jain B., Mo H.J., White S.D.M., 1995, *MNRAS*, 276, L25
Kaiser N., 1987, *MNRAS*, 227, 1
Klypin A., Holtzman J., Primak J., Regős E., 1993, *ApJ*, 416, 1
Klypin A., Primak J., Holtzman J., 1996, *ApJ*, 466, 13
Le Fèvre O., et al., 1996, *ApJ*, 461, 534
Loveday J., Efstathiou G., Peterson B.A., Maddox S.J., 1992, *ApJ*, 400, L43
Loveday J., Maddox S.J., Efstathiou G., Peterson B.A., 1995, *ApJ*, 442, 457
Loveday J., Efstathiou G., Maddox S.J., Peterson B.A., 1996, *ApJ*, in press
Luppino, G., Gioia I., 1995, *ApJ*, 445, L77
Maddox S.J., Efstathiou G., Sutherland W.J., Loveday J., 1990, *MNRAS*, 242, 43P
Maddox S.J., Efstathiou G., Sutherland W.J., 1996, *MNRAS*, in press
Mann R.G., Peacock J.A., Heavens A.F., 1996, *MNRAS*, in preparation.
Ma C.P., Bertschinger E., 1994, *ApJ*, 434, L5
Mo H.J., Jing Y.P., Börner G., 1993, *MNRAS*, 264, 825
Mo H.J., Miralda-Escudé J., 1994, *ApJ*, 430, L25
Mo H.J., Fukugita M., 1996, *ApJ*, 467, L9
Neuschaefer L.W., Windhorst R.A., Dressler A., 1991, *ApJ*, 382, 32
Peacock J.A., 1991, *MNRAS*, 253, 1P
Peacock J.A., Dodds S.J., 1994, *MNRAS*, 267, 1020 (PD94)
Peacock J.A., Dodds S.J., 1996, *MNRAS*, 280, L19 (PD96)
Peebles P.J.E., 1980, *The Large-Scale Structure of the Universe*. Princeton Univ. Press, Princeton, NJ
Pogosyan D.Y., Starobinsky A.A., 1995, *ApJ*, 447, 465
Ratcliffe A., Shanks T., Broadbent A., Parker Q.A., Watson F.G., Oates A.P., Fong R., Collins C.A., 1996, *MNRAS*, 281, L47
Ratra B., Banday A.J., Górski K.M., Sugiyama N., 1996, preprint PUPT-1558
Roche N., Shanks T., Metcalfe N., Fong R., 1993, *MNRAS*, 263, 360
Saunders W., Frenk C., Rowan-Robinson M., Efstathiou G., Lawrence A., Kaiser N., Ellis R., Crawford J., Xia X.-Y., Parry I., 1991, *Nat*, 349, 32
Saunders W., Rowan-Robinson M., Lawrence A., 1992, *MNRAS*, 258, 134
Stompor R., Górski K.M., Banday A.R., 1995, *MNRAS*, 277, 1225
Strauss M.A., Davis M., Yahil Y., Huchra J.P., 1992, *ApJ*, 385, 421
Sugiyama N., 1995, *ApJ Suppl*, 100, 281
Tadros H., Efstathiou G., 1995, *MNRAS*, 276, L45
Tadros H., Efstathiou G., 1996, *MNRAS*, in press
Taylor A.N., Rowan-Robinson M., 1992, *Nat*, 359, 396
Vogeley M.S., Park C., Geller M., Huchra J.P., 1992, *ApJ*, 391, L5
White M., Bunn E.F., 1995, *ApJ*, 450, 477
White S.D.M., Efstathiou G., Frenk C.S., 1993, *MNRAS*, 262, 1023

This paper has been produced using the Royal Astronomical Society/Blackwell Science \TeX macros.